Selective Conjugation of Proteins by Mining Active Proteomes through Click-Functionalized Magnetic Nanoparticles

Shaista Ilyas,[†] Muhammad Ilyas,[‡] Renier A. L. van der Hoorn,[‡] and Sanjay Mathur[†,*]

[†]Institute of Inorganic Chemistry, University of Cologne, Greinstraße 6, D-50939 Cologne, Germany, and [‡]Plant Chemetics Lab, Max Planck Institute for Plant Breeding Research, Carl-von-Linne Weg 10, 50829 Cologne, Germany

ABSTRACT Superparamagnetic iron oxide nanoparticles (SPIONs) coated with azide groups were functionalized at the surface with biotin (biotin@SPIONs) and cysteine protease inhibitor E-64 (E-64@SPIONs) with the purpose of developing nanoparticle-based assays for identifying cysteine proteases in proteomes. Magnetite particles (*ca.* 6 nm) were synthesized by microwave-assisted thermal decomposition of iron acetylacetonate and subsequently functionalized following a click chemistry protocol to obtain biotin and E-64 labeled particulate systems. Successful surface modification and covalent attachment of functional groups and molecules were confirmed by FT-IR spectroscopy and thermal gravimetric analysis. The ability of the surface-grafted biotin terminal groups to specifically interact with streptavidin (either horseradish peroxidase [(HRP)-luminol-H_2O_2] or rhodamine) was confirmed by chemiluminescent assay. A quantitative assessment showed a capture limit of 0.55−1.65 μg protein/100 μg particles. Furthermore, E-64@SPIONs were successfully used to specifically label papain-like cysteine proteases from crude plant extracts. Owing to the simplicity and versatility of the technique, together with the superparamagnetic behavior of FeOx-nanoparticles, the results demonstrate that click chemistry on surface anchored azide group is a viable approach toward bioconjugations that can be extended to other nanoparticles surfaces with different functional groups to target specific therapeutic and diagnostic applications.

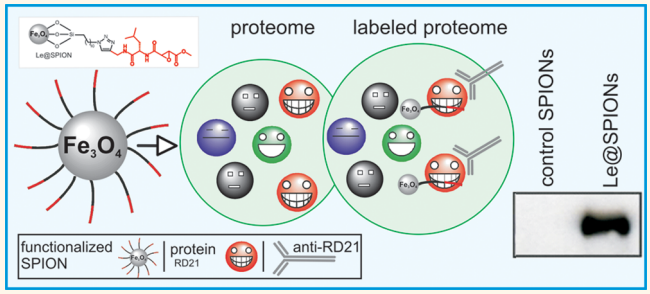

KEYWORDS: microwave-assisted synthesis · click chemistry · iron oxide magnetite nanoparticles · biotin · streptavidin−HRP and rhodamine · cysteine protease inhibitor E-64

The covalent conjugation of biomolecular probes such as proteins to nanoparticles has led to a novel platform of biotargeting and nanoanalytics;[1] however, the retention of protein structure and function in the nano−bio hybrids remains an overarching challenge. The utilization of magnetic iron oxide nanoparticles is mainly derived from their small size and consequent large specific surface area[2−8] crystallinity, superparamagnetism and predominantly a non or minimum dose-dependent cytotoxic behavior.[9] This peculiar combination of attributes opens up broad range of biomedical applications of superparamagnetic iron oxide nanoparticles (SPIONs) including drug carriers,[10] vectors for gene therapy[11] and anticancer therapy through hyperthermia treatment[12] as well as contrast agents (MRI).[5,6,13]

For nanoparticle-based imaging or diagnostic applications, SPIONs are usually conjugated with tagged biological entities for their rapid and site-specific accumulation in regions of interest based on several successful methods derived from click chemistry principles.[14−16] New synthetic protocols to decorate the surface of such particles with biomolecules or target receptors are essential to modulate the coincidental interactions of nanoparticles with bioenvironment ensuring specific attachment.[17,18] For making magnetite particles conducive for biological applications, appropriate surface functionalization enabling covalent immobilization of drug molecules or antibodies as

* Address correspondence to sanjay.mathur@uni-koeln.de.

Received for review May 11, 2013 and accepted October 13, 2013.

Published online October 21, 2013
10.1021/nn402382g

targeting unit toward cell application is essential without influencing the biological function of these molecules.[19] In this context, click chemistry offers a powerful and reliable tool toward the development of functionalized nanomaterials and to label target of interest in biology and medicine.[14,20] The specific and strong binding interaction between biotin and streptavidin that is stable in a wide range of pH and temperature forms the basis for many diagnostic assays and forms a convenient biochemical systems, *e.g.*, in biosensors applications such as high affinity receptor binding.[21,22] Several proteins, such as insulin, pepsin, glucose oxidase, horseradish peroxidase, and fungal protease have been directly conjugated to SPIONs.[23] In most cases, however, the applied strategy had altered the structure and active center of the protein. The advantage of using biotin click chemistry is that it employs suitable reaction conditions, endowing considerable versatility of bioconjugation for a wide variety of biomolecules without reducing their activity.[24] In addition, biotin functionalized SPIONs are suitable for binding with streptavidin bearing modified proteins or antibodies for nanomedicinal applications.[25] Similarly papain-like Cys-proteases (PLCPs) are important biological molecules responsible for plant immunity and their identification is performed with the aid of DCG-04 (biotinylated derivative of cysteine protease inhibitor E-64), which irreversibly reacts with PLCPs when these proteases are active.[26,27] To this end, SPIONs functionalized with protease inhibitor eliminates nonspecific adsorption of other unwanted interfering biomolecules by controlling the surface chemistry of the particles so that proteases can be selectively removed from the crude proteome that eliminates the centrifugation step thereby preventing stress-induced damage to biological materials.[28] In this manuscript, we demonstrate the functionalization of magnetite particles by introducing activity-based probes on the surface of SPIONs. The modified particles enable a fast and efficient way of identifying entire proteome through specific binding and thereby circumventing the multistep co-purification used in the conventional approach.

Given the applicability of click chemistry to surface-attached groups, functionalized SPIONs were synthesized in this work to link biotin and cysteine protease inhibitor E-64. Specifically, SPIONs decorated with azide groups were linked with biotin and cysteine proteases inhibitor E-64 and chemiluminscence and fluorescence scanning methods were used to verify immobilization of biotin on the surface of SPIONs, which confirmed successful surface modifications. Subsequently, E-64@SPIONs were used to capture proteases from crude leaf extracts of *Arabidopsis thaliana* to demonstrate, for the first time, the use of magnetic nanoparticles coated with activity based probes to selectively capture protease from crude proteome. In our system, the protease capturing *via* functionalized SPIONs provides an excellent alternative to handle extensive protein work and this approach could offer significant advantage especially when multiple proteins need to be studied.

RESULTS AND DISCUSSION

Synthesis and Functionalization of Nanovectors. The integration of surface-functionalized SPIONs and click chemistry principles offers a promising approach to specify biomolecular interactions between the surface anchored chemical functionality and target molecules for creating new biodiagnostic assays such as cell-tracking and targeting of biomolecules.[29] Click chemistry on magnetic vectors is a versatile pathway for covalent immobilization of drug molecules, especially for the attachment of targeting moieties in which orientation and stability of linkages are particularly important.[30,31] Furthermore, the SPIONs can be used, after functionalization, to magnetically separate target proteins from crude plant leaf extract (Scheme 1).

The crystal structure of as-synthesized nanoparticles was investigated using powder X-ray diffraction studies (Figure 1B) that confirmed the formation of magnetite nanoparticles of various sizes subject to synthesis time periods. The (311) plane of Fe_3O_4 was used to calculate the mean crystallite size using Scherer's equation, $D = 0.9\ \lambda/\beta \cos\theta$, where D is the particle size, λ is the wavelength of X-ray used, Cu ($\alpha = 0$, 15 406 nm), θ is the half diffraction angle of 2θ, and β is full width at half-maximum. The volumetric average particle size was 6 ± 1 nm, which was supported by transmission electron microscopic analysis (Figure 1A). By varying the synthesis time, we successfully obtained the mean particle sizes of 6 nm (5 min), 9 nm (10 min), and 13 nm (15 min). As-synthesized SPIONs were dispersible in water and largely exhibited single domain character as confirmed by high-resolution TEM analysis (Figure 1A). The particle dispersions in neutral pH range were stable for at least one month when stored at 4 °C in deionized water or phosphate buffer saline (PBS). It was evident from dynamic light scattering that the SPIONs are nanosized and exhibit a narrow size distribution and indeed are compatible with biological buffers (Figure 1D).

As a preliminary step, SPIONs were treated with 11-bromoundecyltrichlorosilane to obtain a Br-terminated surface coverage. The conversion of bromine groups with azide groups was established by a nucleophilic substitution reaction with NaN_3 performed in DMF. For the click part, two biological molecules were used, namely, alkylated biotin and alkylated E-64, which provided two working systems, *i.e.*, biotin@SPIONs (to capture biotin-binding proteins) and E-64@SPIONs (to capture Cys-proteases). E-64 contains a leucine-epoxide reactive group, providing specificity for PLCPs. TEM image investigation of the bromide and azide

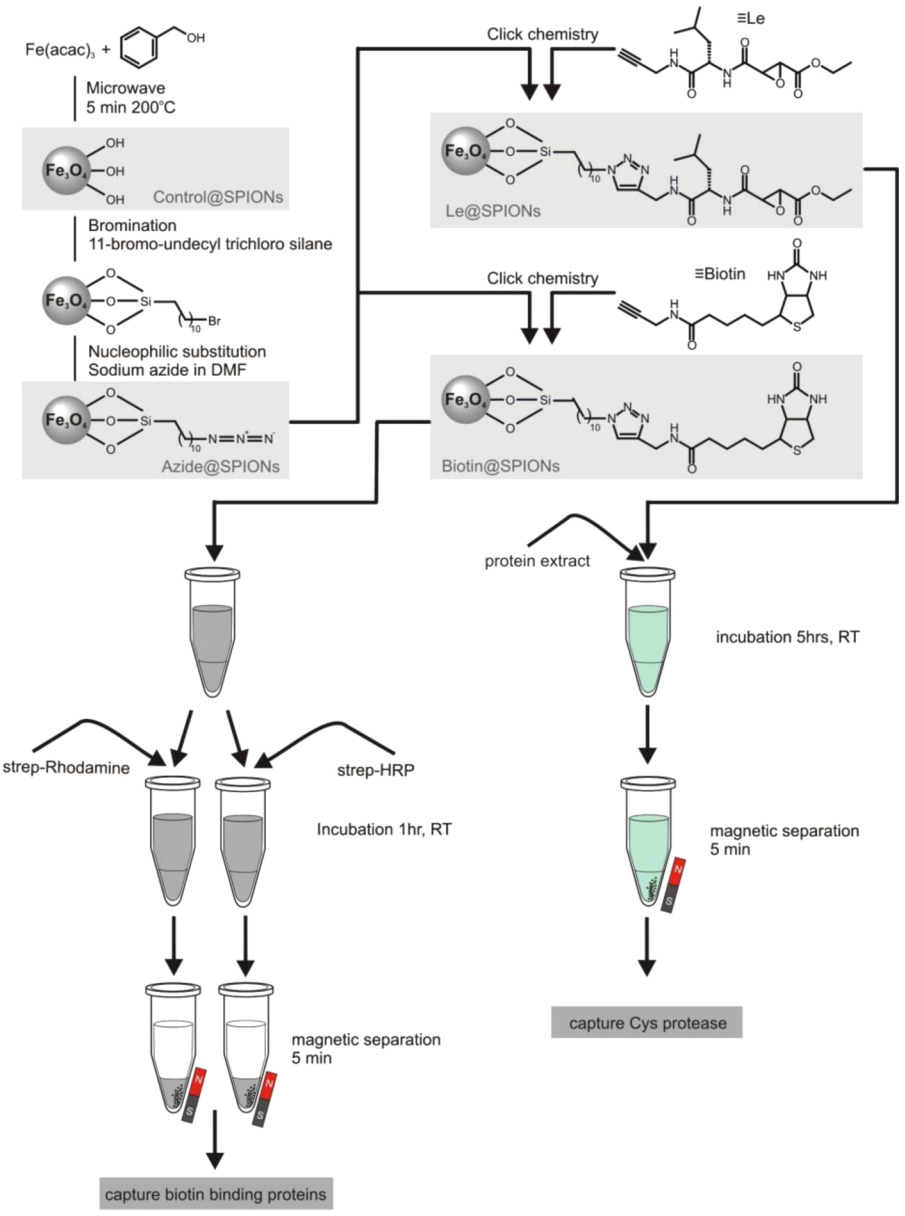

Scheme 1. Schematic representation of the practical steps involved. Microwave assisted synthesis, click chemistry and functionalization of superparamagnetic iron oxide nanoparticles (SPIONs) to capture biotin binding protein and Cys protease in plant proteome. Structure of the alkyne-biotin probe (upper right); structure of the Cys protease inhibitor E-64 containing a leucine-epoxide reactive group provides specificity for PLPCs.

modified SPIONs reveals the organic modified character of SPIONs causing agglomeration whereby nanoparticles showed the same grain size distribution suggesting that surface modification caused no big change on the size and morphology after the click reaction. Attachment of the surface groups evidently altered nanoparticles interaction but primary size (6 ± 1 nm) remained nearly unchanged (Figure 1A). One observable variation is hydrodynamic radius of the nanoparticles, which was significantly larger (*ca.* 38−78 nm) than those found in the TEM analysis and is possibly due to the hydrogen bond formation between the organic groups on adjacent surfaces causing cross-linking between the SPIONs to form larger aggregates. In Br-terminated SPIONs, the hydrodynamic size of the nanoparticles shifted to *ca.* 295 nm apparently due to organic group modification of the nanoparticle surface consequently resulting in the enhancement of hydrodynamic size due to larger polarity (stronger dipole due to the presence of electronegative bromine that will augment H-bonding) of the surface groups. Similarly, hydrodynamic radius of biotin@SPIONs and E-64@SPIONs tends to increase after the click reactions due to more organic groups on the surface of nanoparticles. This suggested that the particles were agglomerated in the medium due to the interaction between organic surface molecules and −OH groups (Figure 1D). The aggregated nature of

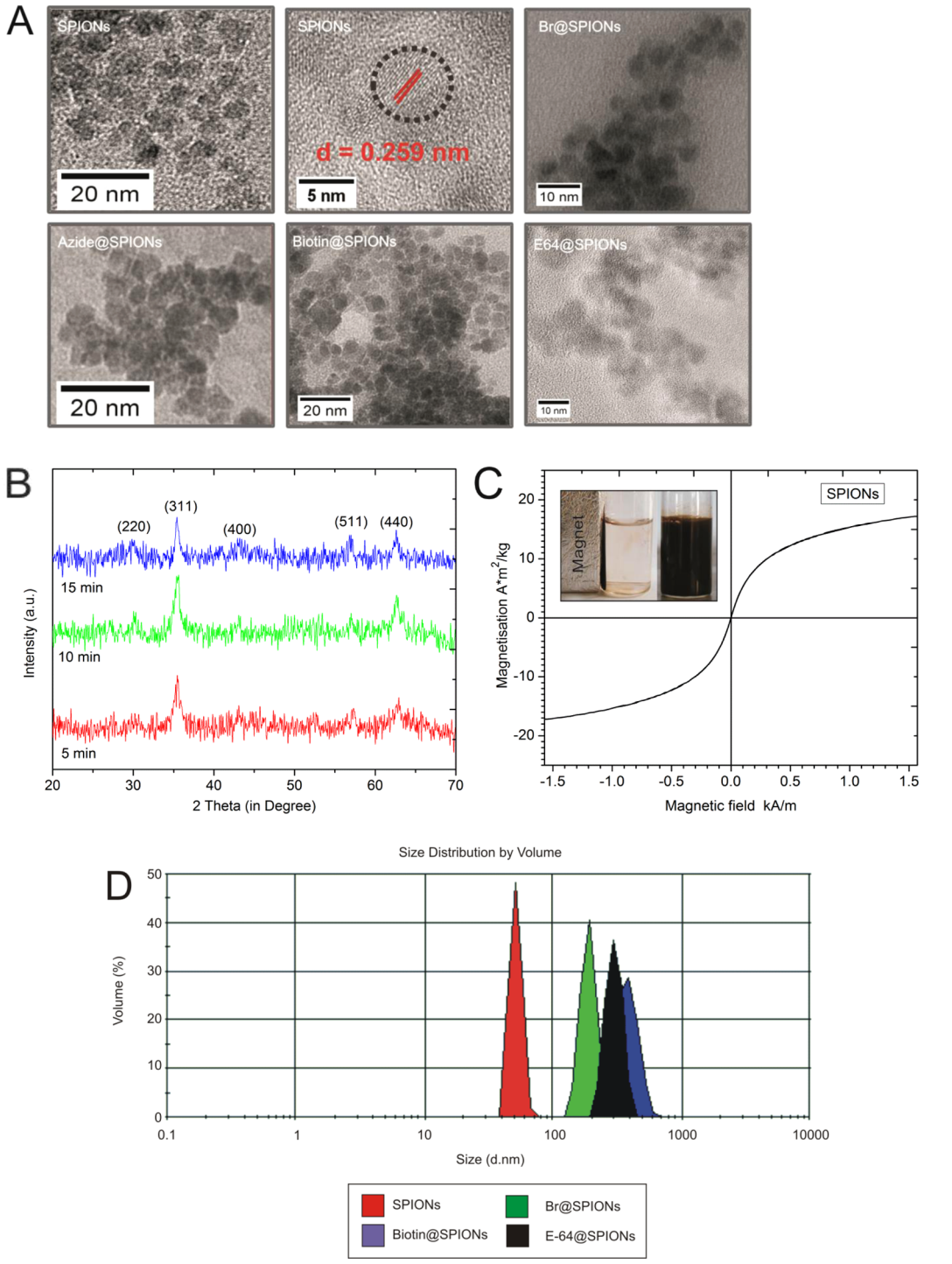

Figure 1. Morphology, crystallinity, magnetization and hydrodynamic size of SPIONs. (A) TEM of spherical SPIONs as synthesized (upper left), HRTEM image with crystalline planes (red) which revealed the highly crystalline nature of SPIONs (upper middle), bromide@SPIONs (upper right), azide@SPIONs (lower left), biotin@SPIONs (lower middle) and E-64@SPIONs (lower right). (B) X-ray diffraction pattern of SPIONs generated at 200 °C at different time points 5, 10, and 15 min. (C) Hysteresis loop of SPIONs shows magnetization curve recorded in applied magnetic field at room temp (inset: magnetic separation). (D) Hydrodynamic size of SPIONs, bromide@SPIONs, biotin@SPIONs and E-64@SPIONs.

particles as indicated by DLS measurements was also observed in TEM images. The magnetic response of these SPIONs was visualized by holding the sample close to a small magnet (Figure 1C, inset). The magnetization curve of the as-synthesized Fe_3O_4 measured at room temperature showed no hysteresis and no saturation indicating their superparamagnetic nature, which is advantageous for many applications such as recyclable catalysis, bioseparation, and controlled drug delivery.

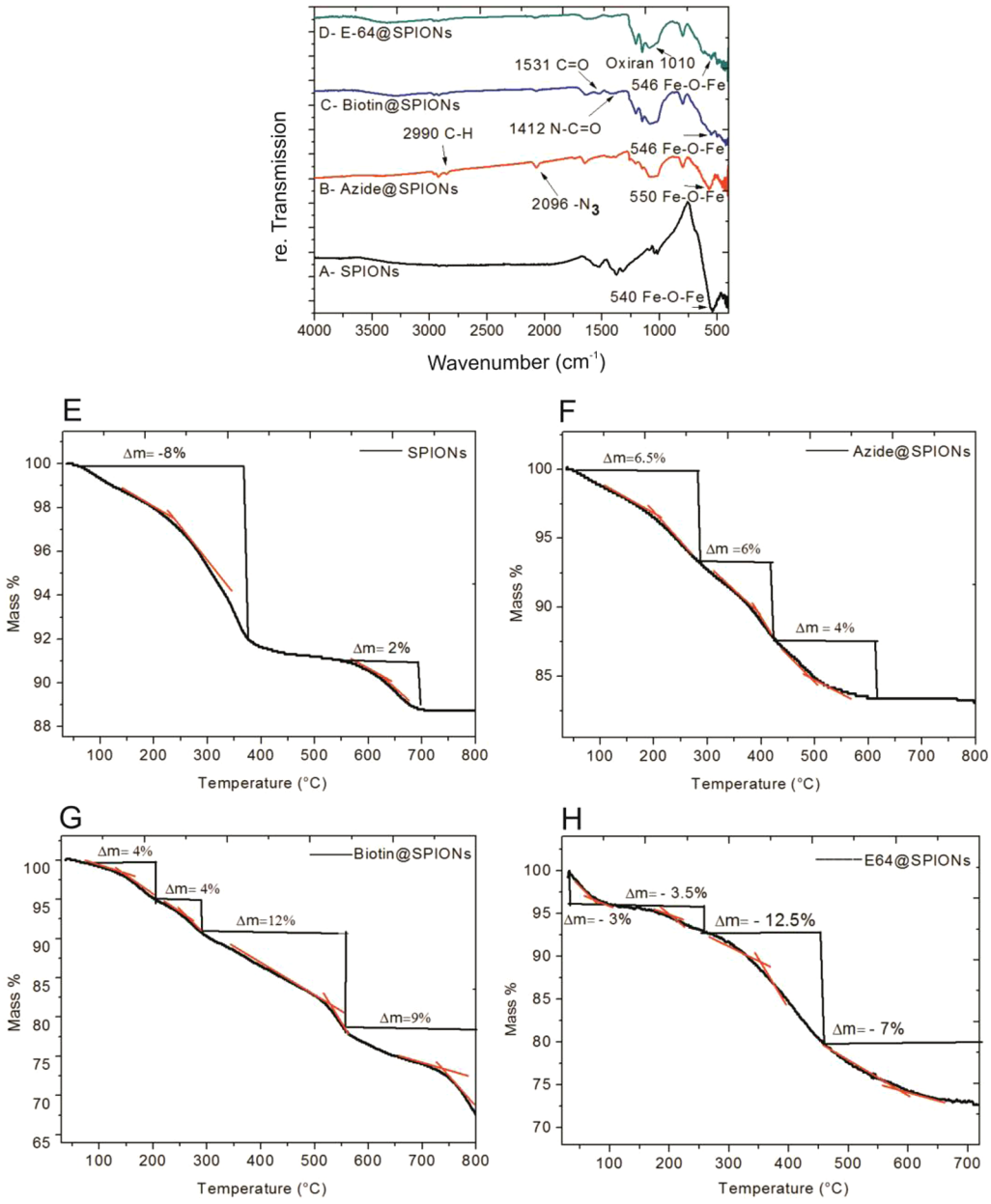

Figure 2. FT-IR and TGA analysis of intermediates used for the functionalization of SPIONs: (A) SPIONs as synthesized (black); (B) azide@SPIONs (red); (C) biotin@SPIONs (blue); (D) Cys protease inhibitor E-64@SPIONs (green) and thermo gravimetric analysis; (E) SPIONs; (F) azide@SPIONs; (G) biotin@SPIONs; (H) E-64@SPIONs.

FT-IR spectra of pure SPIONs exhibited a strong band in the lower wavenumber region (at 540 cm^{-1}) attributed to Fe−O−Fe stretching frequencies (Figure 2A). Upon surface modification with 11-bromoundecyltrichlorosilane and sodium azide, the spectrum was dominated by absorbance bands at 2096 and 2990 cm^{-1} corresponding to the characteristic asymmetric stretching mode of the azide group and C−H stretching frequency, respectively (Figure 2B). The successful occurrence of click reaction was evident in the reduction of azide peaks that was accompanied by the emergence of new peaks at 1412 cm^{-1} assignable to amide II mode (N−C═O) of biotin, while the peak at 1531 cm^{-1} is due to amide I mode (C═O) of biotin (Figure 2C). In a similar manner, the click reaction with alkyne-E64 was verified by the disappearance of the azide peak supported by the epoxy ring peak observed at 1010 cm^{-1} (Figure 2D). After the click reaction, the intensity of Fe−O−Fe vibration at 546 was evidently decreased possibly due to the attachment of organic groups on the surface of SPIONs.[32,33] The inorganic phase of biotin@SPIONs and E-64@SPIONs was identified to be Fe_3O_4 by XRD pattern (Figure S1). Thermal analysis of the modified SPIONs under a nitrogen atmosphere in the temperature range of 30−800 °C and with a 10 °C/min heating rate showed a two-step decomposition process. In the temperature range of 20−381 °C, adsorbed humidity

and protective organic groups on the surface of the nanoparticles were removed. A complete removal of the carbonaceous species was observed at 687 °C with total mass loss being 8% and 2%, respectively. No further weight loss after this point was indicative of the formation of a metal oxide (XRD evidence) of definite composition (Figure 2E). After azide functionalization, thermal characteristics of azide@SPIONs showed four-step decomposition process (Figure 2F), whereby first weight loss at 283 °C and second at 422 °C are indicative of the removal of volatile content and carbonaceous groups on the surface, which is supported by an exothermic event and corresponded to a total weight loss of 12.5%. At 490 °C, additional 4% weight loss was observed possibly due to the removal of residual adsorbed groups present on the nanoparticle surface. After 603 °C, there was no further observable weight loss which confirmed the formation of iron oxide. After click reaction with alkyne-biotin and alkyne-E-64, decomposition behavior of conjugates changed displaying four distinct events indicating a multistep decomposition process involved in the removal of the organic contents present on the surface of nanoparticles. Biotin grafting resulted in two small weight loss events at 198 and 298 °C, respectively, which correspond to a total weight loss of 8% ascribable to the removal of adsorbed water molecules (Figure 2G). A prominent exothermic peak around 565 °C that resulted in *ca.* 12% weight loss is attributed to partial removal of organic shell, which continues until 760 °C and resulted in a further weight loss of 9%. Nanoprobes modified with E-64 showed loss of surface-attached water between 128 and 260 °C, which corresponded to 6.5% weight loss (Figure 2H). The next weight loss of 12.5% is due to the elimination of organic molecules, whereas the last weight loss (7%) is indicative of the removal of residual organics. Biotin@SPIONs showed 3% more weight loss as compared to E-64@SPIONs that can be due to the hydrophilic nature of the biotin as well the particle size-distribution among the different samples. The differential decomposition profiles of various nanoprobes are attributed to the nature (strength) of chemically grafted groups, thermal stability and their interaction with water (*e.g.*, hydrophilic periphery would show more weight loss in the initial temperature range typical for loss of adsorbed water). Finally, the slight deviation in the results is also due to the differing amount of SPIONs present in the samples and the size-distribution of particles present in different probes.

Biodetection Assays with Magnetic Nanovectors. To determine if biotin@SPIONs can capture biotin binding proteins, biotin@SPIONs and control SPIONs (bare SPIONs) were incubated with streptavidin–HRP (horse radish peroxidase) and bovine serum albumin (BSA) at room temperature for 1 h. The particles were washed and incubated with luminol containing chemiluminescence

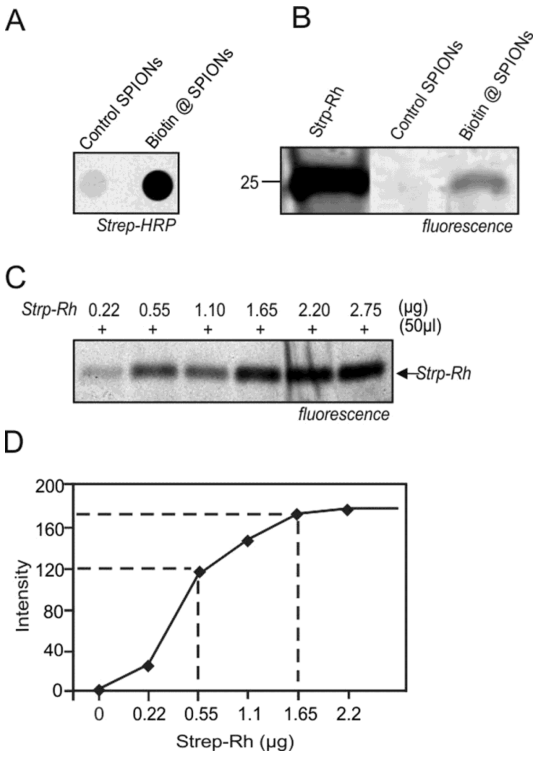

Figure 3. Biotin@SPIONs selectively capture streptavidin–HRP and rhodamine. (A) Biotin@SPIONs was detected with streptavidin–HRP and chemiluminescence. (B) Captured streptavidin–rhodamine was detected with SDS-PAGE electrophoresis. (C) Concentration course of streptavidin–rhodamine using biotin@SPIONs (100 μg). Each mixture of biotin@SPIONs and streptavidin–rhodamine was incubated for 1 h, and maximum emission intensities at 580 nm were recorded after each addition of streptavidin–rhodamine solution. (D) Saturation binding curve determined by quantification of luminescence intensity.

solution to detect HRP activity. Emitted light was recorded using light sensitive films, whereupon a strong chemilumiscence signal was detected for the biotinylated SPIONs (Figure 3A, right). In contrast, no measurable signal was detected for control SPIONs (Figure 3A, left). Similar results were obtained using fluorescent streptavidin incubated with biotin@SPIONs and bare SPIONs (Figure 3B). To get quantitative prospect for the interaction between the biotin@SPIONs and streptavidin, we performed a concentration course assay using fluorescent streptavidin. To obtain clear evidence, 100 μg dispersions of biotin@SPIONs were prepared in PBS, with different concentrations of fluorescent streptavidin ranging from 0.55 to 2.75 μg. After 1 h incubation, beads were washed and eluted by boiling at 95 °C in protein gel loading buffer. The samples were separated on protein gel, and detected by fluorescent scanning. The observed signal intensity proved that capturing 100 μg of biotin@SPIONs required 0.55 μg of fluorescent streptavidin (Figure 3C,D). In summary, we have developed a biotechnological assay technique using clickable-SPIONs and based on biotin–streptavidin interaction. The results of the

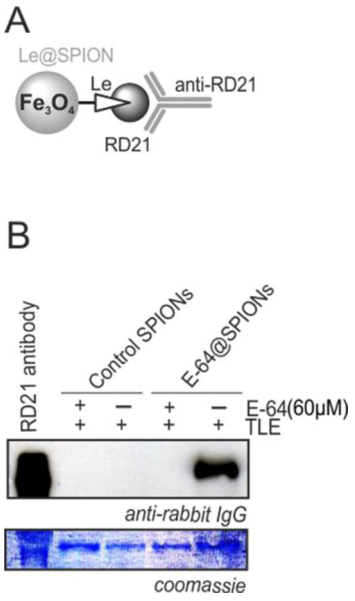

Figure 4. E-64@SPIONs capture of Cys protease RD21 from plant proteome. (A) Schematic representation of capturing and detecting Cys protease RD21 using Le@SPIONs (Leucine-Epoxide E-64). (B) Detection of RD21 antibody captured on E-64@SPIONs incubated with leaf proteome. The eluted proteins were separated on protein gel and analyzed on protein blot using a secondary antibody linked to horseradish peroxidase (HRP) that detects the RD21 antibody. The RD21 was only detected using E-64@SPIONs but not control SPIONs. Lower panel represents the loading control. TLE represents total leaf extract.

present assay can greatly facilitate optimization of experimental conditions for such specific detections in a variety of applications, since biotin functionalized nanoparticles are suitable for binding to streptavidin and modified proteins or antibodies.

To use surface modified SPIONs for other protein capture approaches, E-64, a reversible inhibitor of PLCPs, was used as a specific probe. To examine whether E-64@SPIONs can selectively capture cysteine proteases, a leaf extract of the model plant *A. thaliana* with E-64@SPIONs and control beads (see Experimental Section) was incubated and the captured proteins were analyzed with an antibody against RD21, an abundant cysteine protease in *Arabidopsis* leaf extract.[34] After antibody binding, the beads were washed and boiled in SDS sample buffer and eluted proteins were separated on a protein gel to analyze the protein blot using a secondary antibody that detects the RD21 antibody. The RD21 antibody was only detected using E-64@SPIONs and not by the control beads (Figure 4). Preincubation of leaf proteomes with an excess of E-64 before adding the SPIONs prevented the capture of RD21 on the nanoparticles, thereby demonstrating that capture was specific for Cys proteases. (Figure 4). In summary, we report that specific capture of Cys proteases present in crude leaf extract is possible with functionalized SPIONs. The experimental data shows that this new labeling system is not only useful for specific tracking and targeting of Cys protease, but it can also be extended to other alkylated molecules to target different proteins in a specific system.

CONCLUSIONS

Superparamagnetic magnetite nanocrystals (SPIONs) synthesized by microwave-assisted thermal decomposition of iron(III) acetylacetonate precursor were modified based on click chemistry protocols to successfully introduce bromide and azide groups on their surface. Following the modulation of surface chemistry landscape, the grafted azide groups were utilized to attach biotin and Cys-proteases inhibitor E-64 through click-chemistry protocols. The detection of attached biotin with streptavidin−HRP and Rh conjugates provided a model system for the validation of our initial hypothesis. Furthermore, E-64@SPIONs were successfully applied to capture cysteine proteases from crude leaf extracts that demonstrates the successful utilization of magnetic separation. Additionally, capturing proteases on the functionalized SPIONs significantly simplified the process and it is fast and potentially more target-specific than traditional assays. In general, azide@SPIONs can be used to attach various chemical groups on the surface of SPIONs and to adapt this flexible surface chemistry to separate specific molecules from crude proteomes for developing new biotechnological assays and target specific therapeutic and diagnostic applications.

EXPERIMENTAL SECTION

Materials. Iron acetyl acetonate, [Fe(acac)$_3$], streptavidin−HRP, streptavidin−rhodamine, sodium azide (NaN_3), and *N*,*N*-dimethylformamide (DMF, 99.99%) were purchased from Sigma-Aldrich. Benzyl alcohol (99.5%, Fluka) and 11-bromoundecyltrichlorosilane (95%, $C_{11}H_{22}BrCl_3Si$, ABCR) were also commercially procured. All chemicals were used as received. *A. thaliana* ecotype Columbia was grown in a standard greenhouse at 22 °C under a 16-h light regime. Leaves were obtained from 6 week-old *Arabidopsis* plants. Horseradish-peroxidase-conjugated anti-rabbit antibodies were from Amersham Pharmacia Biotech.

Synthesis of Fe_3O_4 SPIONs Using Microwave Method. Superparamagnetic magnetite nanoparticles were prepared by a microwave-assisted thermal decomposition method based on previous reports and undertaking minor modifications in the procedure.[35] Iron acetylacetonate (1 mmol) was dissolved in 5 mL of benzyl alcohol under an inert atmosphere at room temperature and the resulting solution was transferred into a glass vial (vessel inner volume of 10 mL, sealed with a Teflon cap) and subjected to microwave irradiations operating at 2.45 GHz and 300 W. The solution was treated at 200 °C for 5 min. Upon cooling, the product was magnetically separated and washed several times with absolute ethanol and dried at 60 °C for 6 h. The final black powder was collected for further characterization.

Surface Modification of SPIONs. SPIONs (500 mg) were dispersed in toluene by ultrasonication of suspensions followed by the addition of 250 μL of 11-bromoundecyltrichlorosilane. The reaction mixture was stirred overnight at room temperature.

After centrifugation, it was washed with toluene and alcohol to remove any unbound 11-bromoundecyltrichlorosilane. The retrieved particles were dried overnight at room temperature and treated with 10 mL of saturated solution of sodium azide for 48 h at room temperature in DMF to replace bromide groups present on the surface with azide groups. The resulting suspension was centrifuged and azide-modified particles were washed with acetone and alcohol and dried overnight at room temperature.[36]

Synthesis of Biotin@SPIONs via Click Reaction. For biotinylation, click reaction between azide@SPIONs and alkylated biotin was carried out in a solution prepared by dispersing the azide@SPIONs in toluene (2 mg/mL). The dispersion was added into 1 mL of DMSO solution containing 2 μL of 50 mM alkylated biotin and refluxed under constant stirring for 48 h at 110 °C in mild conditions using $CuSO_4.5H_2O$ as a catalyst. The obtained suspension was centrifuged and biotin modified particles were washed with toluene and dried overnight at room temperature.[37]

Specificity of Biotin@SPIONs Using Streptavidin–Rhodamine Assay. For detection of biotin@SPIONs by streptavidin–rhodamine conjugate, 1 mg of biotin@SPOINs was dispersed in 1 mL of Tris-buffered saline (TBS) containing 3% BSA for 1 h on a rotary shaker at room temperature followed by washing with TBS containing 1% Tween to remove the access BSA. A total of 50 μL of biotin@SPIONs was incubated with streptavidin–rhodamine conjugate (0.5 μL of 1 mg/200 μL PBS) for 1 h on a rotary shaker at room temperature followed by washing with Tris-buffered saline Tween (TBS-T, 3×) to remove unbound streptavidin–rhodamine using an external magnet. Samples were boiled in 50 μL of gel loading buffer to elute the streptavidin–rhodamine. Equal amounts of samples were separated on SDS-PAGE (15% acrylamide) using Novex Minicell system (Invitrogen) at 160 V/250 mA for 70 min. Fluorescent gel was analyzed on typhoon scanner with excitation range of 580 nm.

Scanning and Quantification of Biotin@SPIONs. The amount of streptavidin–rhodamine conjugate required to interact with 100 μg of biotin@ SPIONs was determined by performing a concentration assay. For this purpose, the streptavidin–rhodamine conjugate was reconstituted with PBS (1 mg/200 μL). The dispersed biotin@SPIONs were incubated with different amount of streptavidin–rhodamine conjugate ranging from 0.22 to 2.75 μg for 1 h on a rotary shaker. The blank experiment involved the use of unbiotinylated SPIONs with the addition of 0.55 μg of streptavidin–rhodamine conjugate. Particles were then washed with TBS-T (5×) and separated using external magnet. Standard SDS-PAGE gel electrophoresis was implied (Novex Minicell system, Invitrogen). Fluorescence gel was subjected to wash (5×) with water and the gel was scanned for fluorescence with typhoon scanner with excitation range of 580 nm. The scanned signals were quantified using Image Quant software.

Specificity of Biotin Conjugated SPIONs Using Streptavidin–HRP. For detection of biotin@SPIONs by streptavidin–HRP, the black microtiter plate was used. After removing unbound streptavidin–HRP, samples were poured into the wells of microtiter plate followed by addition of ECL substrate and incubation. The plate was exposed to X-ray films in the dark room and developed by automatic X-ray film processor, when signals were visualized after a short exposure of the microtiter plate.

Synthesis of E-64@SPIONs via Click Reaction. For a click reaction, 10 mg of azide@SPIONs was dispersed in toluene by ultrasonication for 1 h followed by the addition of 1 mL of DMSO containing 2 μL of 50 mM alkylated E-64 in mild conditions using $CuSO_4 \cdot 5H_2O$ as a catalyst . The dispersion was refluxed under constant stirring for 48 h at 110 °C. The product was collected by centrifugation, washed several times with dry toluene, and dried overnight at room temperature.

Protein Extraction from *A. thaliana* Leaves and Western Blot Analysis. One rosette leaf of *A. thaliana* ecotype Columbia (4–6 week-old) was ground with metal beads in 500 μL of water containing 1 mM dithiothreitol (DTT). Samples were centrifuged at 12 000 rpm for 5 min at 4 °C and the supernatant was used for labeling experiments. Preincubation (30 min) was carried out mixing 425 μL of leaf extract with 50 mM sodium acetate, pH 6, 1 mM DTT, and 60 mM E-64 inhibitor to reach a final volume of 500 μL. One milligram of E- 64@SPOINs was dispersed in 1 mL of TBS containing 3% BSA for 1 h on a rotary shaker at room temperature followed by washing with TBS containing 1% Tween to remove the access BSA. The dispersed 50 μL of E-64@SPIONs and uncoated SPIONs (1 mg/500 μL) were added into preincubated samples separately. All samples were incubated under gentle agitation on a rotator (STR4, Stuart) for 5 h. SPIONs were sorted out using external magnet followed by washing with freshly prepared 6 M urea and PBS buffer separately. Washed SPIONs were probed with 1:3000, 3.3 μL primary antibody against RD21 for 1 h under gentle shaking followed by washing with TBS-T. Tris-glycine SDS gel (12% acrylamide) was run to separate the proteins using Novex Minicell system (Invitrogen) at 160 V/250 mA for 70 min. Proteins were transferred onto an Immobilon-P polyvinylidenedifluoride membrane (Immobilon-P, Millipore) using X-Cell II Blot Module system (Invitrogen) at 250 mA for 60 min. After the membrane was blocked with 5% BSA in TBST, residual BSA was removed by TBS-T. The washed membrane was probed with anti-rabbit (1:5000, 1 h shaking) linked to horseradish peroxidase (HRP). The membrane was washed with TBST, and HRP was detected by enhanced chemiluminescence (ECL, Pieice) and recorded by X-ray films.

Instrumentation. FT-IR (Fourier Transform Infrared) spectra were recorded on a Perkin-Elmer-Spectrum 400 with Universal ATR sampling accessory in the range 400–4000 cm^{-1}. The particle size and morphology of SPIONs were determined by LEO 912-Omega, microscope Carl Zeiss, Germany, operating with an accelerating voltage of 120 K eV. The samples were prepared by releasing a drop of ethanol dispersion of particles directly onto the carbon-coated copper grid and drying at room temperature. High resolution electron microscopy of nanocrystals was performed on a Philips CM 300 microscope. Powder X-ray diffractorgrams of nanopowders were recorded on a STOE-STADI MP diffractometer equipped with a Cu (α = 0.15406 nm) source and operating in transmission mode. Magnetization curve was monitored with an ADE Magnetics Vibrating Sample Magnetometer EV7 at room temperature to investigate dependence of sample magnetic moment on applied magnetic field. Samples were measured in sealed Teflon vessel, placed on a glass sample holder between two poles of an electromagnet and vibrated at a frequency of 75 Hz. Quantitative bioassay was carried out in 96 well plates using a commercial chemiluminescent assay system and exposed to X-ray films (Bio Max MR, Kodak) in the darkroom. The exposed film was developed by automatic X-ray film processor (Optimax, Protec) at Max Planck Institute for Plant Breeding Research, Cologne, Germany. Proteins were separated on 12% SDS-PAGE gels and transferred onto polyvinylidene fluoride (PVDF) membrane. Membranes were blocked with 5% (v/w) bovine serum albumin (BSA) in Tris-buffered saline Tween (TBST) for 10 min and incubated for 1 h with anti-rabbit antibody (linked to horseradish peroxidase (HRP)) at a dilution of 1:5000 in blocking solution. The membranes were washed and developed using chemiluminescence (ECL, Pieice). For visualization, an automatic X-ray film processor was used.

Conflict of Interest: The authors declare no competing financial interest.

Acknowledgment. We gratefully acknowledge the financial support and infrastructure provided by the University of Cologne and the Max Planck Society, COST action CM1004 and DAAD-HEC Pakistan. We further extend our thanks to Dr. L. Belkoura, Mr. J. Schlaefer and Mr. O. Arslan for their help with the TEM analysis, Prof. A. Schmidt for magnetization studies, and Dr. C. Gu and Dr. F. Kaschani for fruitful scientific discussions.

Supporting Information Available: XRD data of biotin@SPIONS and E-64@SPIONS. This material is available free of charge *via* the Internet at http://pubs.acs.org.

REFERENCES AND NOTES

1. Amstad, E.; Textor, M.; Reimhult, E. Stabilization and Functionalization of Iron Oxide Nanoparticles for Biomedical Applications. *Nanoscale* **2011**, *3*, 2819–2843.
2. Buerki-Thurnherr, T.; Xiao, L.; Diener, L.; Arslan, O.; Hirsch, C.; Maeder-Althaus, X.; Grieder, K.; Wampfler, B.; Mathur, S.;

Wick, P.; *et al. In Vitro* Mechanistic Study towards a Better Understanding of ZnO Nanoparticle Toxicity. *Nanotoxicology* **2013**, *7*, 402–416.
3. Hirsch, C.; Buerki-Thurnherr, T.; Xiao, L.; Arslan, O.; Wampfler, B.; Mathur, S.; Roesslein, M.; Wick, P.; Krug, H. F. A Comprehensive Evaluation Platform To Assess Nanoparticle Toxicity *in Vitro*. *Toxicol. Lett.* **2012**, *211*, S41.
4. Xia, X. R.; Monteiro-Riviere, N. A.; Mathur, S.; Song, X.; Xiao, L.; Oldenberg, S. J.; Fadeel, B.; Riviere, J. E. Mapping the Surface Adsorption Forces of Nanomaterials in Biological Systems. *ACS Nano* **2011**, *5*, 9074–9081.
5. Xiao, L.; Li, J.; Brougham, D. F.; Fox, E. K.; Feliu, N.; Bushmelev, A.; Schmidt, A.; Mertens, N.; Kiessling, F.; Valldor, M.; *et al.* Water-Soluble Superparamagnetic Magnetite Nanoparticles with Biocompatible Coating for Enhanced Magnetic Resonance Imaging. *ACS Nano* **2011**, *5*, 6315–6324.
6. Kim, B. H.; Lee, N.; Kim, H.; An, K.; Park, Y. I.; Choi, Y.; Shin, K.; Lee, Y.; Kwon, S. G.; Na, H. B.; *et al.* Large-Scale Synthesis of Uniform and Extremely Small-Sized Iron Oxide Nanoparticles for High-Resolution T1Magnetic Resonance Imaging Contrast Agents. *J. Am. Chem. Soc.* **2011**, *133*, 12624–12631.
7. Tromsdorf, U. I.; Bigall, N. C.; Kaul, M. G.; Bruns, O. T.; Nikolic, M. S.; Mollwitz, B.; Sperling, R. A.; Reimer, R.; Hohenberg, H.; Parak, W. J.; *et al.* Size and Surface Effects on the MRI Relaxivity of Manganese Ferrite Nanoparticle Contrast Agents. *Nano Lett.* **2007**, *7*, 2422–2427.
8. Cavelius, C.; Moh, K.; Mathur, S. Chemically Designed Growth of Monodisperse Iron Oxide Nanocrystals. *Cryst. Growth Des.* **2012**, *12*, 5948–5955.
9. Laurent, S.; Burtea, C.; Thirifays, C.; Häfeli, U. O.; Mahmoudi, M. Crucial Ignored Parameters on Nanotoxicology: The Importance of Toxicity Assay Modifications and "Cell Vision". *PLoS One* **2012**, *7*, e29997.
10. Zhao, Z.; Huang, D.; Yin, Z.; Chi, X.; Wang, X.; Gao, J. Magnetite Nanoparticles as Smart Carriers To Manipulate the Cytotoxicity of Anticancer Drugs: Magnetic Control and pH-Responsive Release. *J. Mater. Chem.* **2012**, *22*, 15717–15725.
11. Li, C.; Li, L.; Keates, A. C. Targeting Cancer Gene Therapy with Magnetic Nanoparticles. *Oncotarget* **2012**, *3*, 365–370.
12. Guardia, P.; Di Corato, R.; Lartigue, L.; Wilhelm, C.; Espinosa, A.; Garcia-Hernandez, M.; Gazeau, F.; Manna, L.; Pellegrino, T. Water-Soluble Iron Oxide Nanocubes with High Values of Specific Absorption Rate for Cancer Cell Hyperthermia Treatment. *ACS Nano* **2012**, *6*, 3080–3091.
13. Chung, H. J.; Lee, H.; Bae, K. H.; Lee, Y.; Park, J.; Cho, S. W.; Hwang, J. Y.; Park, H.; Langer, R.; Anderson, D.; *et al.* Facile Synthetic Route for Surface-Functionalized Magnetic Nanoparticles: Cell Labeling and Magnetic Resonance Imaging Studies. *ACS Nano* **2011**, *5*, 4329–4336.
14. Le Droumaguet, B.; Nicolas, J.; Brambilla, D.; Mura, S.; Maksimenko, A.; De Kimpe, L.; Salvati, E.; Zona, C.; Airoldi, C.; Canovi, M.; *et al.* Versatile and Efficient Targeting Using a Single Nanoparticulate Platform: Application to Cancer and Alzheimer's Disease. *ACS Nano* **2012**, *6*, 5866–5879.
15. Wahajuddin; Arora, S. Superparamagnetic Iron Oxide Nanoparticles: Magnetic Nanoplatforms as Drug Carriers. *Int. J. Nanomed.* **2012**, *7*, 3445–3471.
16. El-Gamel, N. E. A.; Wortmann, L.; Arroub, K.; Mathur, S. SiO_2@Fe_2O_3 Core-Shell Nanoparticles for Covalent Immobilization and Release of Sparfloxacin Drug. *Chem. Commun.* **2011**, *47*, 10076–10078.
17. White, M. A.; Johnson, J. A.; Koberstein, J. T.; Turro, N. J. Toward the Syntheses of Universal Ligands for Metal Oxide Surfaces: Controlling Surface Functionality through Click Chemistry. *J. Am. Chem. Soc.* **2006**, *128*, 11356–11357.
18. Boyer, C.; Whittaker, M. R.; Bulmus, V.; Liu, J.; Davis, T. P. The Design and Utility of Polymer-Stabilized Iron-Oxide Nanoparticles for Nanomedicine Applications. *NPG Asia Mater.* **2010**, *2*, 23–30.
19. Colombo, M.; Carregal-Romero, S.; Casula, M. F.; Gutierrez, L.; Morales, M. P.; Bohm, I. B.; Heverhagen, J. T.; Prosperi, D.; Parak, W. J. Biological Applications of Magnetic Nanoparticles. *Chem. Soc. Rev.* **2012**, *41*, 4306–4334.
20. Martin, A. L.; Bernas, L. M.; Rutt, B. K.; Foster, P. J.; Gillies, E. R. Enhanced Cell Uptake of Superparamagnetic Iron Oxide Nanoparticles Functionalized with Dendritic Guanidines. *Bioconjugate Chem.* **2008**, *19*, 2375–2384.
21. Weber, P. C.; Ohlendorf, D. H.; Wendoloski, J. J.; Salemme, F. R. Structural Origins of High-Affinity Biotin Binding to Streptavidin. *Science* **1989**, *243*, 85–88.
22. Pulkkinen, M.; Pikkarainen, J.; Wirth, T.; Tarvainen, T.; Haapa-aho, V.; Korhonen, H.; Seppala, J.; Jarvinen, K. Three-Step Tumor Targeting of Paclitaxel Using Biotinylated PLA- PEG Nanoparticles and Avidin-Biotin Technology: Formulation Development and *in Vitro* Anticancer Activity. *Eur. J. Pharm. Biopharm.* **2008**, *70*, 66–74.
23. Jiang, W.; Xie, H.; Ghoorah, D.; Shang, Y.; Shi, H.; Liu, F.; Yang, X.; Xu, H. Conjugation of Functionalized SPIONs with Transferrin for Targeting and Imaging Brain Glial Tumors in Rat Model. *PLoS One* **2012**, *7*, e37376.
24. Besanceney-Webler, C.; Jiang, H.; Zheng, T.; Feng, L.; Soriano del Amo, D.; Wang, W.; Klivansky, L. M.; Marlow, F. L.; Liu, Y.; Wu, P. Increasing the Efficacy of Bioorthogonal Click Reactions for Bioconjugation: A Comparative Study. *Angew. Chem., Int. Ed.* **2011**, *50*, 8051–8056.
25. Bhaskar, S.; Tian, F.; Stoeger, T.; Kreyling, W.; de la Fuente, J. M.; Grazu, V.; Borm, P.; Estrada, G.; Ntziachristos, V.; Razansky, D. Multifunctional Nanocarriers for Diagnostics, Drug Delivery and Targeted Treatment Across Blood-Brain Barrier: Perspectives on Tracking and Neuroimaging. *Part. Fibre Toxicol.* **2010**, *7*, 3.
26. Richau, K. H.; Kaschani, F.; Verdoes, M.; Pansuriya, T. C.; Niessen, S.; Stüber, K.; Colby, T.; Overkleeft, H. S.; Bogyo, M.; van der Hoorn, R. A. L. Subclassification and Biochemical Analysis of Plant Papain-like Cysteine Proteases Displays Subfamily-Specific Characteristics. *Plant Physiol.* **2012**, *158*, 1583–1599.
27. Shindo, T.; Misas-Villamil, J. C.; Hörger, A. C.; Song, J.; van der Hoorn, R. A. L. A Role in Immunity for Arabidopsis Cysteine Protease RD21, the Ortholog of the Tomato Immune Protease C14. *PLoS ONE* **2012**, *7*, e29317.
28. Veiseh, O.; Gunn, J. W.; Zhang, M. Design and Fabrication of Magnetic Nanoparticles for Targeted Drug Delivery and Imaging. *Adv. Drug Delivery Rev.* **2010**, *62*, 284–304.
29. Xu, C.; Sun, S. Monodisperse Magnetic Nanoparticles for Biomedical Applications. *Polym. Int.* **2007**, *56*, 821–826.
30. Prakash, S.; Long, T. M.; Selby, J. C.; Moore, J. S.; Shannon, M. A. "Click" Modification of Silica Surfaces and Glass Microfluidic Channels. *Anal. Chem.* **2006**, *79*, 1661–1667.
31. Haensch, C.; Hoeppener, S.; Schubert, U. S. Chemical Modification of Self-Assembled Silane Based Monolayers by Surface Reactions. *Chem. Soc. Rev.* **2010**, *39*, 2323–2334.
32. Chouhan, G.; Wang, D.; Alper, H. Magnetic Nanoparticle-Supported Proline as a Recyclable and Recoverable Ligand for the CuI Catalyzed Arylation of Nitrogen Nucleophiles. *Chem. Commun.* **2007**, *0*, 4809–4811.
33. Mazur, M.; Barras, A.; Kuncser, V.; Galatanu, A.; Zaitzev, V.; Turcheniuk, K. V.; Woisel, P.; Lyskawa, J.; Laure, W.; Siriwardena, A.; *et al.* Iron Oxide Magnetic Nanoparticles with Versatile Surface Functions Based on Dopamine Anchors. *Nanoscale* **2013**, *5*, 2692–2702.
34. van der Hoorn, R. A.; Leeuwenburgh, M. A.; Bogyo, M.; Joosten, M. H.; Peck, S. C. Activity Profiling of Papain-like Cysteine Proteases in Plants. *Plant Physiol.* **2004**, *135*, 1170–1178.
35. Bilecka, I.; Djerdj, I.; Niederberger, M. One-Minute Synthesis of Crystalline Binary and Ternary Metal Oxide Nanoparticles. *Chem. Commun.* **2008**, 886–888.
36. Haensch, C.; Hoeppener, S.; Schubert, U. S. Chemical Surface Reactions by Click Chemistry: Coumarin Dye Modification of 11-Bromoundecyltrichlorosilane Monolayers. *Nanotechnology* **2008**, *19*, 035703.
37. Fu, R.; Fu, G.-D. Polymeric Nanomaterials from Combined Click Chemistry and Controlled Radical Polymerization. *Polym. Chem.* **2011**, *2*, 465–475.